JOURNAL OF MATERIALS SCIENCE 30 (1995) 1379–1385

Investigation of equilibrium and phase stability in the liquid/solid state in nickel-based wrought superalloys

G. I. ROSEN
National Laboratory, Materials Department, P.O. Box 49, DK-4000 Roskilde, Denmark

S. F. DIRNFELD, M. BAMBERGER
Technion, Israel Institute of Technology, Department of Materials Engineering, Technion City, Haifa 32000, Israel

B. PRINZ
Metallgesellschaft AG, Metall-Laboratorium, Reuterwlg 14, 60271 Frankfurt am Main, Germany

Isothermal holding experiments between the liquidus temperatures, T_L, and the solidus temperatures, T_S, were carried out on nickel-based wrought superalloys. It was found that during solidification the elements aluminium, cobalt and tungsten tend to dissolve in the γ matrix whereas titanium, tantalum and molybdenum tend to segregate into the liquid. Molybdenum and titanium cause the formation of brittle σ and η phases, respectively, after prolonged holding at elevated temperatures, in accordance with the results of New-PHACOMP (new phase computation).

1. Introduction

Nickel-based wrought superalloys are important materials for service at elevated temperatures in jet engines or in the chemical industry due to their good resistance to corrosion combined with high creep strength. Earlier works [1, 2] investigated the solubility limits of the alloying elements in the Ni–Cr–Al–Ti system. Other works [3–6] concentrated on the solubility limits of aluminium, titanium and molybdenum in the Ni–Cr based alloys. A recent study [7] investigated the maximum solubility of chromium and molybdenum in the γ-Ni phase and the composition of the topologically close packed (TCP) phases beyond the solubility limit in the Ni–Cr–Mo system.

The purpose of the current study was to investigate the liquid/solid equilibrium state and the segregation behaviour of the different alloying elements (i.e. aluminium, titanium, tantalum, cobalt, tungsten, molybdenum) in some experimental nickel-based wrought superalloys by simulating ingot solidification.

2. Experimental procedure

2.1. Alloy selection, preparation and experimental methods

The alloy compositions which were chosen for this investigation can be seen in Table I. In addition, the alloys contain negligible residual amounts of iron, manganese, silicon, carbon, oxygen, nitrogen, zirconium, niobium, cobalt and sulphur. The preparation stages included: vacuum induction melting and casting of 50 kg square (50×50 mm) ingots, solution treating, hot rolling and homogenization followed by hot forming to rods of 12 mm diameter.

The liquidus and the solidus temperatures (T_L and T_S, respectively) of the alloys were determined by utilizing the differential thermal analysis (DTA) method. Bulk samples, 12 mm diameter and a few centimetres long, were placed in an alumina crucible in the furnace. The samples were protected by a flow of 99.99% pure argon gas. The experiments were performed at several temperatures between the liquidus temperature and the solidus temperature. These stages consisted in solution treating inside the furnace by holding the samples at a temperature of 20 °C above the liquidus temperature for 2 h, rapidly cooling the samples to a temperature in the liquidus/solidus range and holding for 22 h followed by water quenching.

The different phases which formed in the alloys as a result of the various thermal treatments were identified by means of X-ray diffraction. Samples preparation stages included machining to platelets 1 mm thick and 10 mm diameter, rough primary polishing on TiC abrasive polishing paper, and surface electro-polishing etching.

The microstructure was investigated using a scanning electron microscope equipped with an energy dispersive spectrometer (EDS) for local composition analysis. Sample preparation stages included rough polishing on TiC carbide abrasive paper, smoothing on rotating wheels covered with diamond paste, and electrical etching.

0022–2461

TABLE I Alloys compositions (wt %)

Alloy	Ni	Cr	Al	Ti	Ta	Co	W	Mo
32	77.7	19.1	1.6	1.6	–	–	–	–
35	74.4	20.0	5.6	–	–	–	–	–
36	79.6	19.1	–	1.3	–	–	–	–
37	76.9	19.0	1.7	2.4	–	–	–	–
72	74.2	17.1	2.1	2.5	3.0	1.1	–	–
73	74.3	16.0	2.1	2.6	3.0	1.0	1.0	–
74	73.3	16.1	2.0	2.5	3.0	2.0	1.1	–
75	65.5	15.9	2.1	2.5	–	10.0	1.9	2.1
76	63.9	15.9	2.1	2.5	1.5	10.0	2.0	2.1
77	62.5	16.0	2.0	2.5	2.9	10.0	2.0	2.1

TABLE II M_d for various elements

Element	M_d level (eV)
Ti	2.271
V	1.543
Cr	1.142
Mn	0.957
Fe	0.858
Co	0.777
Ni	0.717
Cu	0.615
Zr	2.944
Nb	2.117
Mo	1.550
Hf	3.020
Ta	2.224
W	1.655
Re	1.267
Al	1.900
Si	1.900

TABLE III Alloys liquidus and solidus temperatures

Alloy	T_S (°C)	T_L (°C)	$\Delta T_{L\,S}$ (°C)
32	1370	1385	15
35	1352	1366	14
36	1391	1403	12
37	1352	1368	16
72	1323	1358	35
73	1330	1363	33
74	1318	1351	33
75	1347	1382	35
76	1335	1371	36
77	1322	1362	40

2.2. Computer analysis

New-PHACOMP is a program for predicting precipitation of brittle TCP phases in nickel-based superalloys [8–11]. It was developed on the basis of theoretical calculations of electronic structures by the discrete variation X_α cluster method. Accordingly, a mathematical model for the phase precipitation relationship between γ and γ' was developed [9]. In alloyed Ni_3Al with transition elements, new energy levels due to the d-orbitals of alloying elements, appear above the Fermi level. For the 4d and 5d transition elements, such new levels appear and change systematically with the order in the periodic table of the elements. These metal d levels (M_d) correlate with electronegativity and are related to the metallic radius of element M as well. The average value of M_d in alloys designated $\bar{M}_d$ and defined as the compositional average of the values of all alloying elements, is calculated as follows [10, 11]

$$\bar{M}_d = \sum_{i=1}^{n} X_i(M_d)_i \quad (1)$$

where, X_i is the atomic fraction of component i in the alloy, and $(M_d)_i$ is the M_d value for component i. The summation is taken over all the components, $i = 1, 2, \ldots, n$. The values of M_d for various transition metals and copper, aluminium and silicon are listed in Table II [11]. It is assumed that when the $\bar{M}_d$ becomes larger than a certain value, phase instability takes place and the second phase occurs in the γ matrix. Several studies [12, 13] have derived an empirical equation to calculate critical $\bar{M}_d$ for the formation of σ-phase in nickel-based superalloys

$$\text{Critical } \bar{M}_d = 6.25 \times 10^{-5}\, T(\text{K}) + 0.834 \quad (2)$$

where T is the absolute temperature. The temperature coefficient can be compared with the coefficient of thermal energy, $kT = 8.62 \times 10^{-5}\, T$ eV, where k is the Boltzmann constant.

In the current investigation, New-PHACOMP was employed in order to predict the formation of the brittle σ-phase out of the frozen residual liquid during holding at elevated temperature. The program input contains the different element concentrations in the residual liquid, at the different temperatures between liquid and solid. The output is the values of $\bar{M}_d$. If these values exceed the above critical $\bar{M}_d$ (in accordance to the temperature), there is a danger of σ-phase formation.

3. Results

The values of the liquidus and solidus temperatures (T_L and T_S, respectively) are listed in Table III. Water quenching of the samples at the end of each isothermal holding experiment resulted in the "freezing" of the equilibrium structure between the liquidus and the solidus at the given temperature, and transformed the liquid phase into a fine dendritic structure. A typical example can be seen in Fig. 1. In most cases, the samples were held in three different temperatures between liquidus and solidus. The equilibrium

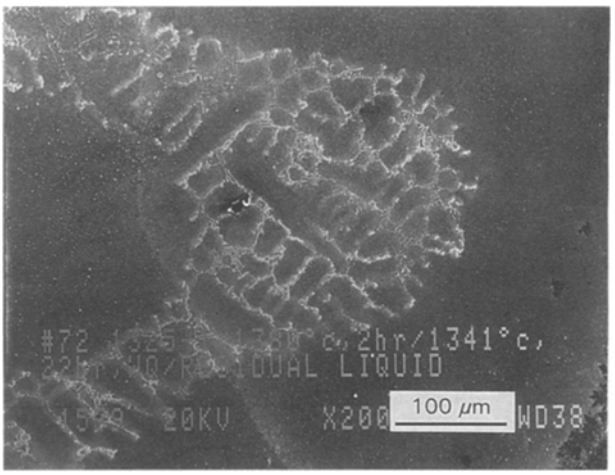

Figure 1 Typical microstructure of alloy 72 after isothermal holding. Experimental stages consisted of solution for 2 h at 1378 °C, isothermal holding for 22 h at 1341 °C, and water quenching. The white dendritic area is the frozen residual liquid.

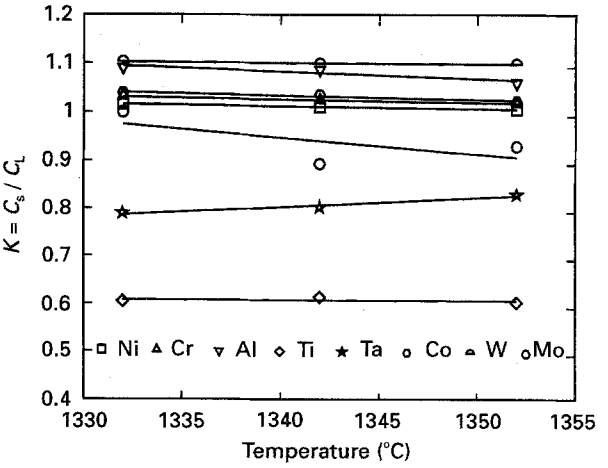

Figure 3 The partition coefficient, K, as a function of temperature for all the elements in alloy 77. (□) Ni, (△) Cr, (▽) Al, (◇) Ti, (☆) Ta (⬡) Co, (⏢) W, (○) Mo.

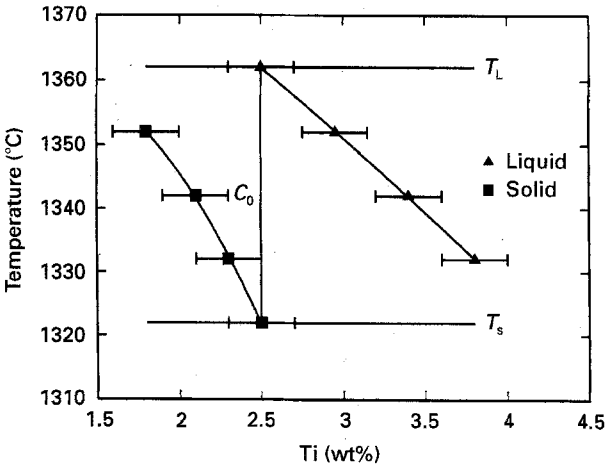

Figure 2 Frozen residual (▲) liquid and (■) primary solid concentration as a function of temperature for titanium in alloy 77.

concentrations of the primary solid which precipitates, C_S, the frozen residual liquid, C_L, and the nominal concentrations, C_0 at each temperature were determined by employing EDS while examining the samples in the SEM. In order to achieve better accuracy in the measurements, each C_S and C_L point represents an average of ten EDS measurements. Fig. 2 shows an example of one of the alloying elements (e.g. titanium) concentrations as a function of temperature in alloy 77. Similar graphs were plotted for all the other elements in the alloys. The segregation tendencies of the different elements in the alloys can easily be described via the partition coefficient, $K = C_S/C_L$. Fig. 3 shows all K results at the various isothermal holding temperatures for the elements in alloy 77. It can be seen that molybdenum, tantalum and titanum segregate into the liquid (i.e. $K < 1$) whereas the solid is enriched with nickel, chromium, cobalt, aluminium and tungsten (i.e. $K > 1$).

The results of the New-PHACOMP in the frozen residual liquid show that in alloys 32, 35, 36, 37, 72, 73 and 74 there is no danger of σ-phase formation. On the other hand, in alloys 75, 76 and 77 the New-PHACOMP results in the frozen residual liquid predict formation of σ-phase. An example of the calculation results for alloys 37, 72 and 76 is shown in Table IV. In order to verify the results of the predictions of the New-PHACOMP, all the alloys were subjected to an additional thermal treatment for 600 h at 900 °C (following the primary isothermal holding stage at the different temperatures). Identification of the different phases formed out of the frozen residual liquid was performed by SEM and XRD. A typical example, representing the series of alloys 32, 35, 36 and 37 can be seen in Fig. 4. Only γ′ precipitates were observed. The X-ray spectrum of this series in Fig. 5 shows that only γ′-phase, M_7C_3 carbides and $M_{23}C_6$ carbides, were formed. A typical example, representing the series of alloys 72, 73 and 74 can be seen in Fig. 6. Needle-like brittle η-phase and carbides which were formed along grain boundaries were observed. The X-ray spectrum of this series in Fig. 7 shows that, in addition to formation of the γ′-phase and carbides, the brittle η-phase is formed. A typical example, representing the series of alloys 75, 76 and 77 can be seen in Fig. 8. This exhibits plate-like brittle σ-phase nucleated from $M_{23}C_6$ carbides at grain

TABLE IV New-PHACOMP results

Alloy	Iso. temp. (°C)	Residual liquid comp. (wt %) Ni	Co	Cr	Mo	W	Ta	Ti	Al	$\bar{M}_d$ (eV)	Critical $\bar{M}_{d(900°C)}$
37	1357	75.80	–	20.40	–	–	–	2.65	1.15	0.848	0.907
72	1341	73.05	0.65	17.25	–	–	4.10	3.75	1.20	0.858	0.907
76	1353	63.90	9.35	15.80	1.90	2.0	1.75	3.35	1.95	0.912	0.907

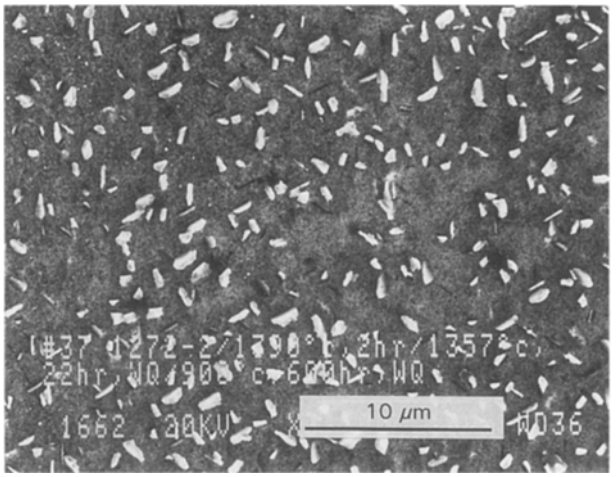

Figure 4 Representative microstructure of the alloys series 32, 35, 36 and 37. Experimental stages consisted of solution at 1388 °C for 2 h, isothermal holding between liquidus and solidus at 1357 °C for 22 h, water quenching and ageing at 900 °C for 600 h. Alloy 37, shown here, exhibits randomly dispersed γ′-phase precipitates.

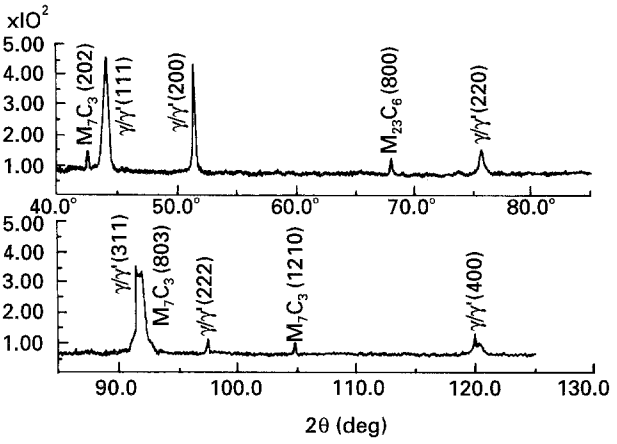

Figure 5 X-ray spectrum of the alloy in Fig. 4. Only the γ′-phase and M_7C_3 and $M_{23}C_6$ carbides were identified.

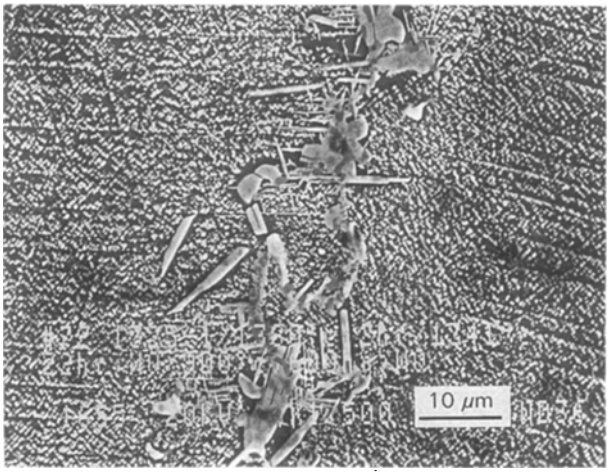

Figure 6 Representative microstructure of the alloy series 72, 73 and 74. Experimental stages consisted of solution at 1378 °C for 2 h, isothermal holding between liquidus and solidus at 1341 °C for 22 h, water quenching and ageing at 900 °C for 600 h. Alloy 72, shown here, exhibits needle-like brittle η-phase and carbides which were formed along grain boundaries.

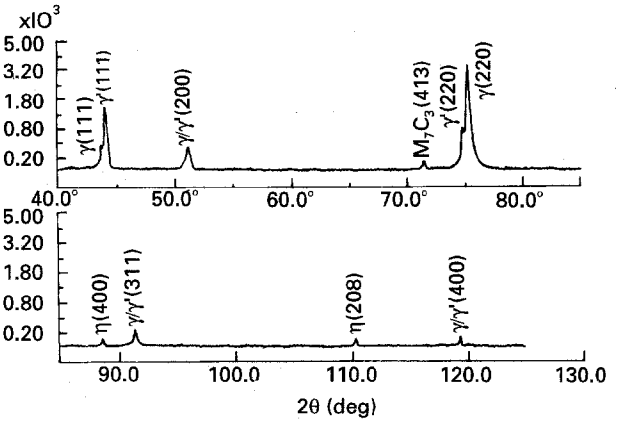

Figure 7 X-ray spectrum of the alloy in Fig. 6. The γ′-, η- and carbide phases were identified.

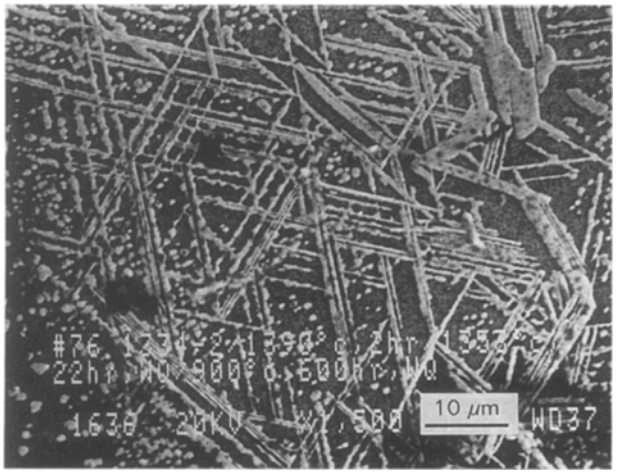

Figure 8 Representative microstructure of the alloy series 75, 76 and 77. Experimental stages consisted of solution at 1391 °C for 2 h, isothermal holding between liquidus and solidus at 1353 °C for 22 h, water quenching and ageing at 900 °C for 600 h. Alloy 76, shown here, exhibits plate-like brittle σ-phase.

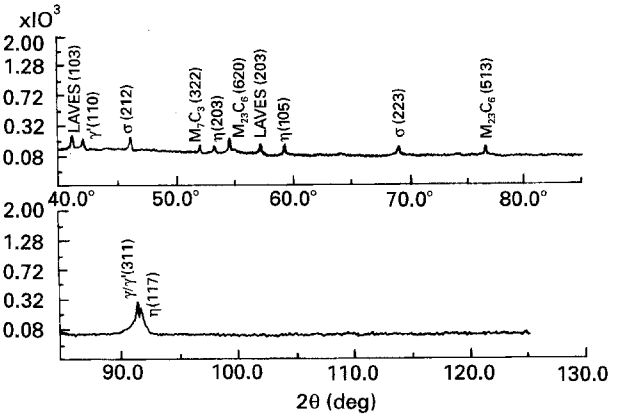

Figure 9 X-ray spectrum of the alloy in Fig. 8. The γ′-, η-, σ-, Laves and carbide phases were identified.

boundaries. The X-ray spectrum of this series in Fig. 9 shows that, in addition to formation of the γ′-phase and carbides, the brittle η-, σ- and Laves phases were formed.

TABLE V K values of the different alloys

Alloy	Ni	Cr	Al	Ti	Ta	Co	W	Mo
32	> 1	> 1	< 1	< 1				
35	> 1	> 1	< 1					
36	> 1	> 1		< 1				
37	> 1	> 1	< 1	< 1				
72	> 1	> 1	> 1	< 1	< 1	> 1		
73	> 1	> 1	> 1	< 1	< 1	> 1	> 1	
74	> 1	> 1	> 1	< 1	< 1	> 1	> 1	
75	> 1	> 1	> 1	< 1		> 1	> 1	< 1
76	> 1	> 1	> 1	< 1	< 1	> 1	> 1	< 1
77	> 1	> 1	> 1	< 1	< 1	> 1	> 1	< 1

4. Discussion

4.1. Tendencies of segregation and solution of the alloying elements

The partition coefficient, K, yields information about the tendencies of the different alloying elements to segregate during solidification. When $K > 1$, the elements tendency is to enrich the primary solid, and when $K < 1$ the elements tendency is to enrich the residual liquid. Table V lists the K values relative to unity of the different alloys.

The precipitation tendencies of the alloying elements is determined mostly by their ability to dissolve into the γ-Ni matrix. According to the classical theories [14, 15] the differences in electronegativity and the atomic size between the solute and the solvent element are the criteria which determine the solubility extent. From these investigations it was found that a difference of ± 0.4 units in electronegativity and $\pm 15\%$ in the atomic size between the solute and the solvent are the criteria for the ability to dissolve. The crystallographic structure is also of an importance, namely, the solvent element preferentially will dissolve an element with a crystallographic structure resembling its own. All these criteria are summarized in Table VI. By adopting these criteria, the behaviour of each element in the matrix can be explained.

$K_{Ni} > 1$ in all the alloys and it is also observed that usually K_{Ni} remains almost constant in the temperature range between the liquidus and the solidus. Moreover, the values of K_{Ni} are similar in the different alloys, and do not depend on their different alloying level.

From Table VI it is seen that the chromium and cobalt are the closest to nickel of all the other alloying elements (e.g. in atomic diameter and in electronegativity) and therefore will tend to dissolve into the nickel matrix. A similar picture (as in the case of nickel) can be described regarding $K_{Cr} > 1$ and $K_{Co} > 1$ in all the alloys. Here, also K_{Cr} and K_{Co} values are similar in all alloys. Gozlan *et al.* [7] have shown that $K_{Cr} = 1$ in all their alloys; however, the values found by us are very close to unity. The discrepancy can be related to the higher alloying level of the alloys investigated in the current research.

Tungsten and molybdenum are rather on the borders of the above-mentioned criteria and therefore their tendency to dissolve in the matrix or to segregate to the liquid is not certain. However, in all cases it was found that $K_W > 1$ and again K_W values are similar in all the alloys. The molybdenum is added only to alloys 75, 76 and 77 in small quantities and in all of them it is found that $K_{Mo} < 1$. Gozlan *et al.* [7] showed that in the Ni–Mo–Fe, Ni–Mo–Cr and Ni–Mo–Fe–Cr systems, molybdenum tends to segregate to the liquid, regardless of its concentration or of the other elements concentrations in the alloy.

According to the criteria for titanium and tantalum in Table VI, they will tend to segregate to the liquid. In all the alloys it was found that $K_{Ti}, K_{Ta} \ll 1$, regardless of the concentration of the other elements. Usually the values of K_{Ta} were somewhat larger than those of K_{Ti}, which means that the nickel matrix extracts more titanium than tantalum.

The aluminium which has the same crystallographic structure as the nickel (i.e. f c c) is the main element for forming the γ′-Ni_3Al phase. According to Table VI the aluminium will tend to dissolve in the solid solution, as indeed was found in most cases. However, in the series of alloys 32–37 it was found that although $K_{Al} < 1$, it is close to unity. This is probably due to insufficient measuring accuracy of the aluminium concentrations, because in all the other alloys it was found that $K_{Al} > 1$, regardless of the other elements concentrations.

4.2. Formation of brittle phases

The New-PHACOMP predicts for alloys 32, 35, 36 and 37 that even in the frozen residual liquid there is

TABLE VI Differences in atomic diameter and electronegativity of the alloying elements compared to nickel

Alloying element	Crystallographic structure	Difference in atomic diameter from Ni (%)	Difference in electronegativity from Ni
Cr	BCC	+ 0.3	− 0.25
Al	FCC	+ 15	− 0.30
Ti	HCP	+ 16	− 0.37
Ta	BCC	+ 15	− 0.41
Co	FCC	+ 0.8	− 0.03
W	BCC	+ 10	+ 0.45
Mo	BCC	+ 9	+ 0.25
B	Rhombohedral	− 22	+ 0.13
C	Diamond	− 38	+ 0.64
Cb	BCC	+ 15	− 0.31
Zr	HCP	+ 27	− 0.58

no danger of the formation of the brittle σ-phase during prolonged service at elevated temperatures (see example in Table IV, in reference to Fig. 4). SEM and X-ray examinations of these alloys (Figs 4 and 5, respectively) show that only the γ- and γ′-phases exist, namely, the computer program predictions are correct.

The New-PHACOMP for alloys 72, 73 and 74 predicts that even in the frozen residual liquid there is no danger for σ-phase to form (see example in Table IV, in reference to Fig. 6). However, SEM and X-ray examinations (Figs 6 and 7, respectively) reveal the existence of the γ- and γ′-phases and the formation of the brittle η-phase. The failure of the computer program to predict the formation of this brittle phase is due to the fact that the program is designed to calculate the tendency of formation of the σ-phase which, in turn, determines the critical $\bar{M}_d$ value. Moreover, in this series, there was no molybdenum addition which is an essential element for the formation of the σ-phase. Furthermore, the γ′-phase, which grows during ageing, is very unstable when it contains higher concentrations of titanium and transforms to the needle-like η-phase. This phenomenon is also enhanced when there is a higher ratio of Ti:Al in the liquid [16]. This was also observed by us (see Fig. 6), e.g. in alloy 72 the nominal ratio of Ti:Al is 2:1, while in the quenched residual liquid from 1332 °C the ratio is 3.3:1.

The New-PHACOMP predictions for the frozen residual liquid in alloys 75, 76 and 77 agree the best with the findings (see example in Table IV, in reference to Fig. 8). The SEM and X-ray results (Figs 8 and 9, respectively) reveal formation of the brittle σ- and η-phases in all this series, because the liquid is enriched with molybdenum.

4.3. Designing proposals of superalloys

The most important engineering requirement in designing an optimal alloy is a stable microstructure during creep and its corrosion resistance.

The current content of chromium in the alloys is justified because it dissolves well in the matrix and expands its lattice parameter (therefore it is a good solid-solution strengthening element). Also, chromium is known for its good ability to form a Cr_2O_3 protective layer.

Tungsten shows that it is not influenced by the presence of other alloying elements in the matrix and therefore in its current content in the alloys contributes to strengthening and does not segregate to grain boundaries.

Compared to this, the molybdenum, which has the same role as the tungsten, is very undesirable in the alloys. Molybdenum tends to segregate to the residual liquid during solidification and causes instability in the interdendritic microstructure. This localized instability results in the formation of the brittle σ-phase after slow cooling of large ingots [17]. This phase can hardly be removed by homogenization and hence its formation must be eliminated by proper alloy design. The molybdenum is hardly dissolved into the γ′ phase and therefore in order to design a better alloy it is recommended to substitute the molybdenum by tungsten. From our findings it is seen that the cobalt is completely dissolved into the matrix and is not influenced by the presence of other alloying elements. However, its atomic mismatch with the nickel is small (+0.8%) and therefore does not contribute much to the solid-solution strengthening mechanism. In addition to the molybdenum, the cobalt enhances the formation of the σ-phase [16, 18] and therefore the relatively high content of cobalt in the alloys is not justified.

The aluminium which is an important element in the formation of the γ′ phase, is justified in its current content level in the alloys. It is well dissolved in the matrix and during ageing reacts with the nickel to form Ni_3Al.

Compared to this, titanium tends, during solidification, to segregate strongly into the residual liquid with no connection to the concentrations of other alloying elements. This tendency causes a higher ratio of Ti:Al in the residual liquid and in turn, promotes the formation of the brittle η-phase. Titanium is essential in the formation of TiC; nevertheless, its tendency to segregate into the liquid is very undesirable. However, it was shown [19] that titanium enhances growth of γ′ precipitates and therefore it is recommended to keep its content to a minimum level in the alloys.

The alloying content of tantalum in the alloys is justified, even though $K_{Ta} < 1$, because it is known that the tantalum does not participate in reactions which form the TCP phases [16]. Our EDS examinations did not reveal substantial contents of tantalum in the σ- and η-phases. Furthermore, tantalum is essential, because it is active in the formation and growth of γ′-Ni_3 (Al, Ti, Ta) precipitates and increases their volume fraction [19, 20].

5. Conclusions

During solidification, the elements aluminium, cobalt and tungsten tend to dissolve in the γ matrix, whereas titanium, tantalum and molybdenum tend to segregate into the liquid. Molybdenum and titanium cause the formation of brittle σ- and η-phases, respectively, after prolonged service at elevated temperatures.

Acknowledgement

The research was promoted by the Federal Ministry for Research and Technology, Bonn, within the programme "German-Israel Cooperation in the field of High-Temperature Materials" (Project 03 M 3003 A7).

References

1. A. TAYLOR and R. W. FLOYD, *J. Inst. Met.* **81** (1952–1953) 451.
2. A. TAYLOR, *J. Met.* **8** (1956) 1356.
3. N. C. OFORKA and B. B. ARGENT, *J. Less-Common Met.* **114** (1985) 97.
4. S. CHAKRAVORTHY, S. SADIQ and D. R. F. WEST, *J. Mater. Sci. Technol.* **2** (1986) 110.
5. N. C. OFORKA and C. W. HAWORTH, *Scand. J. Met.* **16** (1987) 184.

6. P. WILLEMIN and M. DURAND-CHARRE, *J. Mater. Sci.* **25** (1990) 168.
7. E. GOZLAN, M. BAMBERGER, S. F. DIRNFELD, B. PRINZ and J. KLODT, *Mater. Sci. Eng.* **A141** (1991) 85.
8. W. J. BOESCH and J. S. SLANEY, *Met. Prog.* **86** (1964) 109.
9. L. R. WOODYATT, C. T. SIMS and H. J. BEATTIE Jr, *Trans. AIME* **236** (1966) 519.
10. M. MORINAGA, N. YUKAWA, H. ADACHI and H. EZAKI, in "Proceedings of the 5th International Symposium on Superalloys", edited by M. Gell, Seven Springs, Champion, PA, USA, 7–11 October 1984 (AIME, Warrendale, 1984) p. 523.
11. M. MORINAGA, N. YUKAWA, H. EZAKI and H. ADACHI, *Philos. Mag. A* **51** (1985) 223.
12. J. R. MIHALISIN and D. L. PASQUINE, in 'Proceedings of the International Symposium on Structural Stability in Superalloys", Seven Springs, PA, Vol. 1 (1968) p. 134.
13. O. H. KRIEGE and J. M. BARIS, *Trans. ASM* **62** (1969) 195.
14. L. DARKEN and G. W. GURRY, "Physical Chemistry of Metals" (McGraw-Hill, New York, 1953) p. 86.
15. W. HUME-ROTHERY and G. V. RAYNOR, "Structure of Metals and Alloys" (Institute of Metals, London, 1954).
16. C. T. SIMS, N. S. STOLOFF and W. C. HAGEL, "Superalloys II – High Temperature Materials for Aerospace and Industrial Power" (Wiley, New York, 1987).
17. E. GOZLAN, M. BAMBERGER, S. F. DIRNFELD and B. PRINZ, *J. Mater. Sci.* **27** (1992) 3869.
18. J. K. TIEN and R. N. JARRETT, in "Proceedings of Conference on High Temperature Alloys for Gas Turbines", edited by R. Brunetaud, Liege, Belgium, 4–6 October 1982 (Reidel, Dordrecht, 1982) p. 423.
19. G. I. ROSEN, S. F. DIRNFELD, M. BAMBERGER and B. PRINZ, *High Temp. Mater. Proc.* **12** (1993) 183.
20. *Idem, Z. Metallkde* **85** (1994) 127.

Received 16 February 1993
and accepted 17 August 1994